Available online at www.sciencedirect.com
SCIENCE DIRECT
Polymer 47 (2006) 5669–5677
polymer
www.elsevier.com/locate/polymer

Effects of high molecular weight component on crystallization of polyethylene under shear flow

Y. Ogino, H. Fukushima, G. Matsuba, N. Takahashi, K. Nishida, T. Kanaya *

Institute for Chemical Research, Kyoto University, Uji, Kyoto-fu 611-0011, Japan

Received 15 January 2005; received in revised form 25 August 2005; accepted 29 August 2005
Available online 11 May 2006

Abstract

Crystallization of polyethylene (PE) blends of low and high molecular weight components under shear flow was studied using time-resolved depolarized light scattering (DPLS), focusing on effects of the high molecular weight component on the shish–kebab structure formation. Anisotropic two-dimensional scattering pattern due to shish-like structure formation was observed above a certain concentration of the high molecular weight PE. The threshold was about 2.5–3 times larger than the chain overlap concentration, suggesting an important role of entanglements of the high molecular weight component. On the basis of these results a gel-spinning-like mechanism for the shish-like structure formation has been proposed. The DPLS results also implied that the shish-like structure was mainly formed from the high molecular weight PE. This was confirmed by small-angle neutron scattering (SANS) and small-angle X-ray scattering (SAXS) measurements on an elongated PE blend of low molecular weight deuterated PE and high molecular weight hydrogenated PE (3 wt%).

Keywords: Crystallization under flow; Shish–kebab; High molecular weight component

1. Introduction

It is well known [1–6] that when polymers in melts and solutions are crystallized under flows such as elongational and/or shear flows the so-called shish–kebab structure is formed, which consists of long central fiber core (shish) surrounded by lamellar crystalline structure (kebab) periodically attached along the shish. It is believed that the shish is formed by crystallization of completely stretched polymer chains and the kebabs are folded chain lamella crystals and grow to the direction normal to the shish. The shish–kebab structure is very important from industrial viewpoint [7–9] because it is structural origin of ultra-high strength and ultra-high modulus fiber. Among flexible polymers, only ultra-high modulus polyethylene fiber is already available in industry but not for other flexible polymers. One of the reasons is that formation mechanism of the shish–kebab structure is not fully understood. Once we know the basic mechanism we could produce ultra-high modulus fibers for other flexible polymers, and hence elucidation of the formation mechanism is very important.

On the basis of recent developments of advanced characterization techniques, extensive studies have been performed on polymer crystallization under various kinds of flows using in situ rheo-small-angle and wide-angle X-ray scattering (SAXS and WAXS) [10–20] and in situ rheo-small-angle light scattering (SALS) [21–23] and rheo-optical measurements [24–26]. Despite the extensive studies, the formation mechanism of the shish–kebab structure is not fully understood. One of the reasons is that there are many factors, which influence the formation of the shish–kebab structure such as molecular weight, molecular weight distribution, branching in chain, shear rate, shear strain, crystallization temperature and so on. It is necessary in such situation to perform systematic studies on crystallization processes as a function of each factor to elucidate the formation mechanism.

In a previous paper [27], we studied crystallization of polyethylene under shear flow focusing on effects of the shear rate and shear strain. In the present work, we have investigated effects of high molecular weight (HMW) component on the shish–kebab formation under shear flow. There are already some papers reporting effects of HMW component on crystallization under flow [20,28–32]. Most of the results indicated that HMW component or long chains enhanced

* Corresponding author. Tel.: +81 774 38 3140; fax: +81 774 38 3146.
E-mail address: kanaya@scl.kyoto-u.ac.jp (T. Kanaya).

0032-3861/$ - see front matter © 2006 Elsevier Ltd. All rights reserved.
doi:10.1016/j.polymer.2005.08.102

crystallization in the rate and the orientation. Recently, Kornfield et al. [32] have studied effects of HMW component using model blends of HMW isotactic polypropyrene (M_w = 923,000) and low molecular weight (LMW) one (M_w = 186,000), both of which had rather narrow molecular weight distributions, and found that the role of the HMW component in shear-induced crystallization is cooperative, enhanced by entanglements among the long chains. Hsiao and co-workers [20] also demonstrated the role of the HMW component in blends of noncrystallizing low molecular weight polyethylenes (M_w = 50,000 and 100,000) and crystallizing HMW polyethylene (PE) (M_w = 250,000) using in situ rheo-SAXS and rheo-WAXD techniques. The results indicated that the high molecular weight component dominated formation of crystallization precursor structure in the blend under shear flow, and the viscosity of the matrix (low molecular weight component) played an important role to influence the formation of crystallization precursor structure.

In this experiment, we have performed depolarized light scattering measurements on crystallization processes of blends of HMW PE (M_w = 2,000,000) and LMW PE (M_w = 58,600) under shear flow to study effects of the HMW component on the shish–kebab structure formation. In addition, to confirm that the shish structure is mainly formed from the HMW component, we performed small-angle neutron scattering (SANS) and small-angle X-ray scattering (SAXS) measurements on an elongated blend of HMW hydrogenated PE (M_w = 2,000,000) and low molecular weight deuterated PE (M_w = 200,000).

2. Experimental

2.1. Materials

In DPLS studies we used two polyethylenes (PE) with molecular weight M_w = 58,600 and 2,000,000 and the polydispersity M_w/M_n = 8.01 and 12, respectively, where M_w and M_n are the weight- and number-average molecular weight, respectively. The LMW PE was kindly supplied by Showa Denko Ltd, and the HMW PE by Mitsui Chem. Co., Ltd. The nominal melting temperatures of the LMW and HMW PEs determined by DSC measurements were 134 and 135 °C at a heating rate of 20 °C/min. It should be noted that the molecular weight distributions of the PEs are broad, which may smear effects of the high molecular weight component on the shish–kebab formation. However, the large molecular weight difference [M_w(HMW)/M_w(LMW) ~ 34] may overcome the difficulty.

HMW and LMW PEs were dissolved in xylene with anitoxidant regent (2,6-*tert*-butyl-*p*-cresole) to form a homogeneous solution at 130 °C under nitrogen atmosphere. Concentration of the HMW component was in a range of 0.2–3 wt%. After keeping the solution at 130 °C for 1 h, it was quenched into ice/water to precipitate as a gel, filtered from xylene and washed with methanol several times. The gel was vacuum-dried at 70 °C for 2 days and then hot-pressed at 165 °C for 5 min and quenched rapidly to ice/water to get a thin film ~0.3 mm thick. The LMW PE film was prepared under the same procedure as a control sample. In the DPLS measurements, a thin film was placed between two quartz plates, which protected the sample from oxidation, and the thickness was controlled at 0.3 mm before applying the shear. Note that each film was used only once for a measurement to avoid damage due to oxidation or degradation.

For SANS and SAXS measurements, we used HMW hydrogenated PE with M_w = 2,000,000 and M_w/M_n = 12 and LMW deuterated PE with M_w = 200,000 and M_w/M_n = 5. The HMW PE is the same PE as in the DPLS measurements. Strips of the blend film of HMW hydrogenated PE (3 wt%) and LMW deuterataed PE (97 wt%), which was prepared in the same procedure as the DPLS samples, were elongated about six times at a rate of 30 s^{-1} at 133 °C just below the nominal melting temperature (= 135 °C) and quenched to ice/water. These elongated strips were aligned on the cell window. It is noted that the quenching of the blends was done as rapidly as possible to avoid segregation [33–35]. However, in this work we did not check the segregation directly.

2.2. DSC measurements

DSC measurements were carried out to characterize thermal properties of the sample using Perkin–Elmer DSC-7. All the DSC scans were performed under nitrogen environment.

2.3. DPLS measurements

Two-dimensional (2D) depolarized light scattering (DPLS) measurements were carried out using a home-made apparatus with He–Ne laser (80 mW, wavelength λ = 633 nm) as a light source and a CCD camera with 2D screen as a detector system. The range of length of scattering vector Q in this experiment is 4×10^{-5} to 2.6×10^{-4} $Å^{-1}$, where Q is given by $Q = (4\pi \sin\theta)/n\lambda$ (2θ and n being scattering angle and the refractive index, respectively).

A Linkam CSS-450 high temperature shear cell with quartz windows was used to control temperature and shear conditions. Sample thickness was 0.3 mm for all the DPLS measurements. The temperature protocol for the shear experiments is shown in Fig. 1: (a) heat the polymer sample from room temperature to

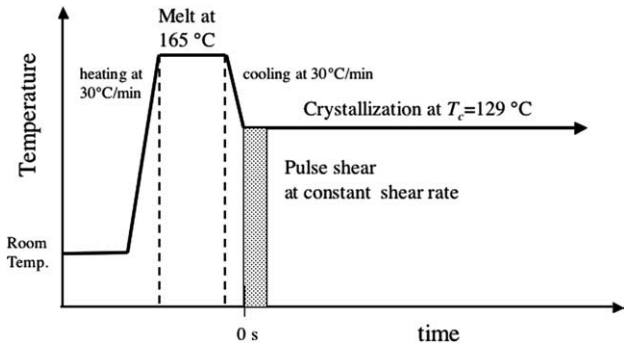

Fig. 1. Temperature protocol for the shear experiments on polyethylene.

165 °C at a rate of 30 °C/min, (b) hold at 165 °C for 5 min, (c) cool down to the crystallization temperature $T_c = 129$ °C at a rate of 30 °C/min, and (d) hold the temperature at 129 °C for the DPLS measurements. The polymer melt was subjected to pulse shear just after reaching the crystallization temperature T_c of 129 °C.

2.4. SANS measurements

Small-angle neutron scattering (SANS) measurements were performed with SANS-U spectrometer [36] at the JRR-3M reactor in Japan Atomic Energy Research Institute (JAERI), Tokai, Japan. Neutron wavelength λ in this measurement was 7 Å with the dispersion $\Delta\lambda/\lambda$ of 10%. Scattered neutrons were detected by a two-dimensional position sensitive detector having 65×65 cm^2 (128×128 pixels) area. In the measurements, we covered a range of magnitude of scattering vector Q ($=4\pi \sin\theta/\lambda$; λ and 2θ being neutron wavelength and scattering angle, respectively) from 0.005 to 0.13 Å^{-1}.

2.5. SAXS measurements

Small-angle X-ray scattering (SAXS) measurements were carried out with an small-angle scattering apparatus installed at the beam line BL45XU [37] in the synchrotron radiation facility, SPring-8, in Nishiharima, Japan. Wavelength of incident X-ray was 0.9 Å and scattered X-ray was detected by a two dimensional CCD camera with an image intensifier. The Q range covered in this measurement was 0.009–0.15 Å^{-1}.

3. Results and discussion

3.1. Depolarized light scattering measurements

First of all, we would like to discuss structure development of LMW PE (matrix PE) during the crystallization process after applying pulse shear. This will give a basis for interpretation of the results of the PE blends. It should be noted that in the present DPLS experiments, we focus our attention on the very early stage of the crystallization, where the scattering intensity is very weak. We therefore, used samples 0.3 mm thick, which are too thick to investigate the late stage due to multiple scattering. Therefore, in the discussion of the DPLS results we concentrate on the results in the early stage.

Fig. 2 shows an example of the time evolution of 2D DPLS pattern for the LMW PE during the crystallization process for the shear rates of 1, 8 and 16 s^{-1}. The shear strain was 3200% for all the measurements. After a certain induction period for the structure formation, we observed isotropic 2D DPLS pattern for the shear rate $\dot{\gamma}$ of 1 s^{-1}. The induction period becomes shorter with increasing the shear rate although the 2D pattern is isotropic, showing acceleration of the crystallization rate with increasing the shear rate. As the shear rate further increases, the 2D scattering pattern becomes anisotropic above about $\dot{\gamma} = 6$ s^{-1} in addition to the acceleration of the crystallization rate. For example, the 2D pattern for $\dot{\gamma} = 16$ s^{-1} shows streak-like scattering normal to the flow direction in the early stage as seen in the lowest row in Fig. 2. The streak-like scattering means that long scattering objects are aligned along the flow direction, which must be a shish structure or a precursor of the shish-structure. At the moment it is not easy to mention if the streak-like scattering is

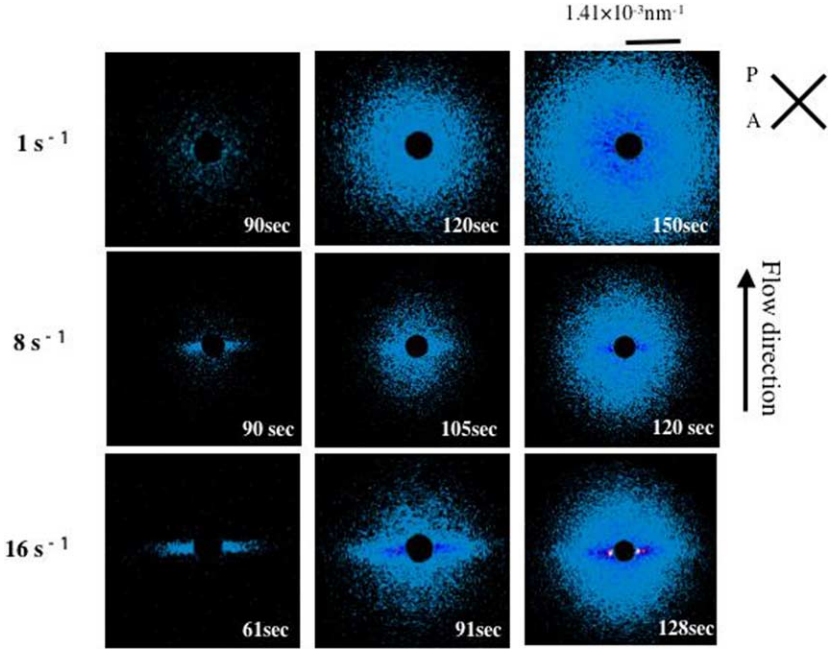

Fig. 2. Time evolution of 2D DPLS patters form the matrix PE (LMW PE) during the crystallization process at 129 °C after pulse shear with shear rates $\dot{\gamma}$ of 1, 8 and 16 s^{-1} from top to bottom. The shear strain ε was 3200%.

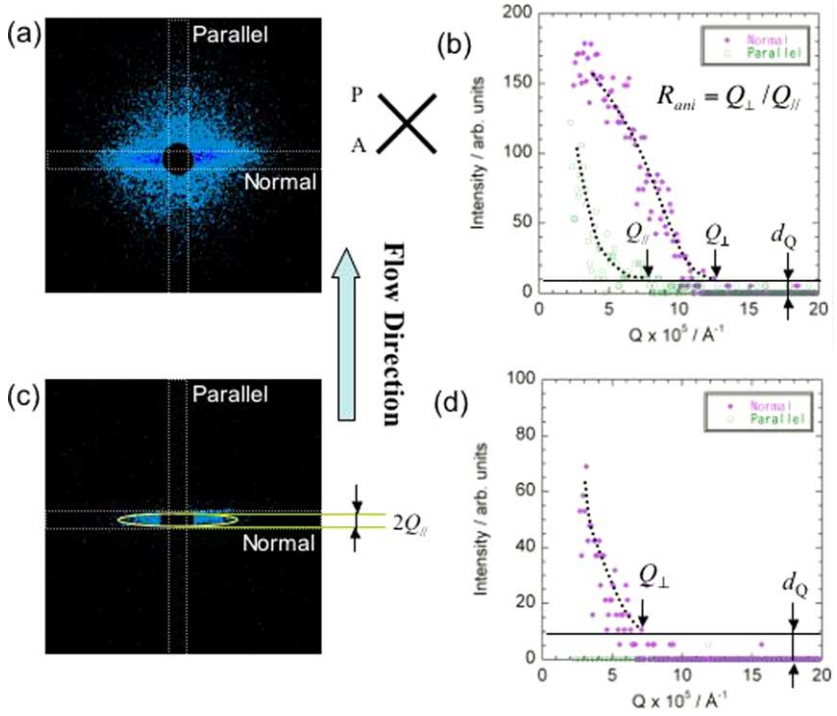

Fig. 3. (a), (c) Typical 2D DPLS patterns, and (b), (d) the definitions of the degree of anisotropy R_{ani} ($=Q_\perp/Q_{||}$) corresponding to (a) and (c), respectively.

caused by the shish or the precursor, and hence termed the shish-like structure in this paper hereafter. Further annealing, the isotropic scattering emerges and covers the anisotropic scattering. In order to evaluate the anisotropy of the 2D scattering pattern quantitatively we have defined a measure for the anisotropy. A typical 2D anisotropic scattering pattern is shown in Fig. 3(a) and the scattering intensities normal and parallel to the flow direction are plotted against Q in Fig. 3(b), respectively. The scattering intensities are very weak in the high Q range while they begin to increase at a certain onset Q values in the low Q range, depending on the scattering direction. We have defined a ratio of the onset Q value normal to the flow direction to the parallel one ($=Q_\perp/Q_{||}$) as a measure of anisotropy, and termed the degree of anisotropy R_{ani} in this paper. The degree of anisotropy R_{ani} is time-dependent: it has a maximum in the early stage and decreases with annealing time. We have employed the maximum value of R_{ani} for the discussion of the degree of anisotropy in this paper.

The maximum value of the degree of anisotropy R_{ani} is plotted as a function of shear rate at various shear strains in Fig. 4 for the matrix PE. In the low shear rate region, the value of R_{ani} is unity, meaning that the scattering is isotropic, and begins to increase at a critical shear rate $\dot{\gamma}$, which depends on the shear strain. For example, the degree of anisotropy R_{ani} is unity below the shear rate of 6 s^{-1} and begins to increase at around 6 s^{-1} for the shear strain ε of 3200%. On the basis of the results, we adopted such shear condition for the experiments of the PE blend that the matrix PE does not show anisotropic scattering pattern. If we observe anisotropic scattering pattern in the PE blend during the crystallization we can directly attribute to effects of the HMW PE.

Fig. 5 shows the time evolution of 2D DPLS patterns of the matrix PE and the PE blend including 3 wt% HMW one during the crystallization process after pulse shear at 129 °C. The shear rate $\dot{\gamma}$ and the shear strain ε are 4 s^{-1} and 1600%, respectively. In the case of the matrix PE isotropic scattering pattern appears at around 80 s after applying the pulse shear and increases in intensity with annealing time. On the other hand, the 3% blend shows very sharp streak-like scattering normal to the flow direction, which appears at around 30 s after the pulse shear, corresponding to the shish-like structure. At about 80 s in the late stage, isotropic scattering appears to cover the anisotropic one. The onset time of the isotropic component in the 3% blend is very close to that in the matrix PE,

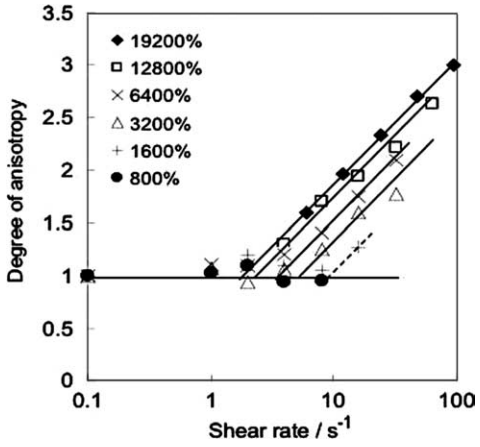

Fig. 4. Shear rate dependence of the degree of anisotropy R_{ani} for the matrix PE (LMW PE) at various shear strains ε from 800 to 19,200%.

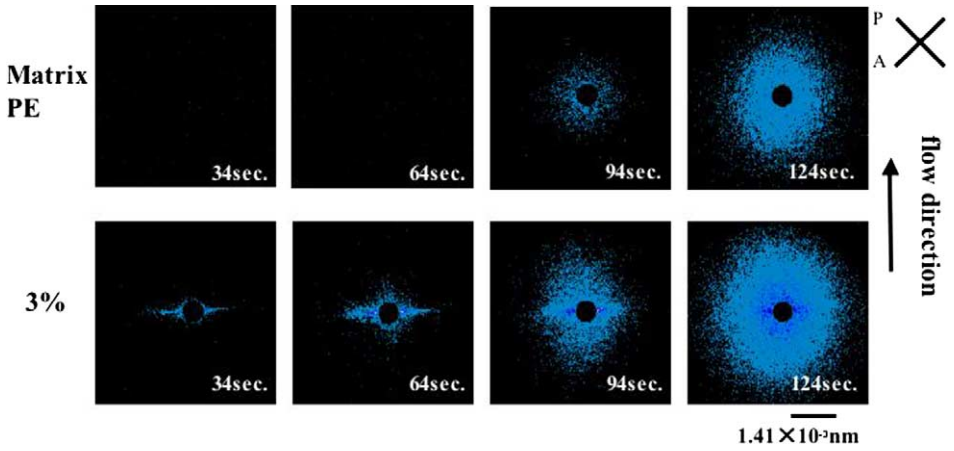

Fig. 5. Time evolution of 2D DPLS patters for the matrix PE (LMW PE) and the PE blend including 3 wt% HMW PE during the crystallization process at 129 °C after pulse shear. The shear rate $\dot{\gamma}$ and the strain were ε 4 s^{-1} and 1600%, respectively.

suggesting that the isotropic scattering in the blend is coming from the matrix PE. On the other hand, it is evident that the streak-like scattering is due to the HMW PE because the matrix PE does not show any anisotropic scattering under this shear condition. From these observations, we can directly conclude that the HMW component enhances the formation of the shish-like structure.

In the next step, we have examined effects of concentration of the HMW PE C_{HMPE} on the degree of anisotropy. Fig. 6 shows the 2D scattering patterns of the PE blends at 68 and 98 s after the pulse shear as a function of the concentration C_{HMPE}. The shear rate and the shear strain were 4 s^{-1} and 3200%, respectively. Anisotropic scattering patterns were not observed when the concentration C_{HMPE} of the HMW PE was less than 0.5 wt%. At around C_{HMPE} = 0.5 wt%, very weak anisotropic scattering was observed at 68 s after the pulse shear as seen in Fig. 6 and the 2D scattering intensity increases in the anisotropy with the concentration C_{HMPE}, suggesting that there is a threshold concentration C^*_{ani} for the anisotropic scattering at around C_{HMPE} = 0.5 wt%. This will be discussed quantitatively later. It should be noted that we showed 2D patterns at 68 s after the pulse shear in Fig. 6 because the anisotropy was the highest at around this time at any concentrations above C_{HMPE} = 0.5 wt%. After the onset of the anisotropic scattering, the isotropic scattering appears at around 80 s after the pulse shear and covers the anisotropic scattering. It is interesting to point out that the onset time of the isotropic scattering, which must come from the LMW PE, is almost independent of the concentration below C_{HMPE} = 0.5 wt%, suggesting that the HMW PE hardly affects the crystallization process of the LMW PE below around C_{HMPE} = 0.5 wt%. On the other hand, the isotropic scattering slightly increases in intensity and the onset time becomes shorter with increasing the concentration C_{HMPE} above C_{HMPE} = 0.5 wt%.

In Fig. 7, the degree of anisotropy R_{ani} at 68 s after the pulse shear is plotted against the concentration of the HMW PE C_{HMPE} for three shear conditions, under which the matrix PE does not show the anisotropic scattering pattern. It is obvious that the degree of anisotropy is almost unity below C_{HMPE} = 0.5–0.6 wt% while it abruptly increases above this

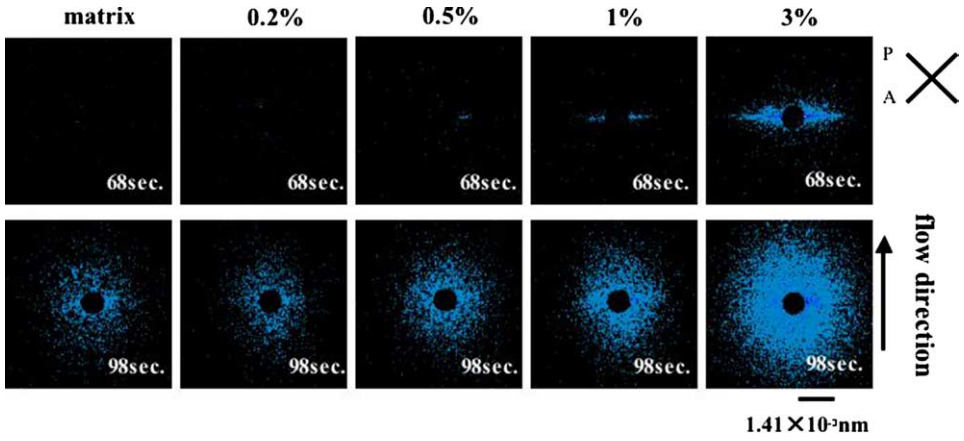

Fig. 6. 2D DPLS patters of the PE blends with various concentrations of the HMW PE from 0 to 3 wt% at 68 and 98 s after pulse shear. The shear rate $\dot{\gamma}$ and the strain were ε 4 s^{-1} and 1600%, respectively.

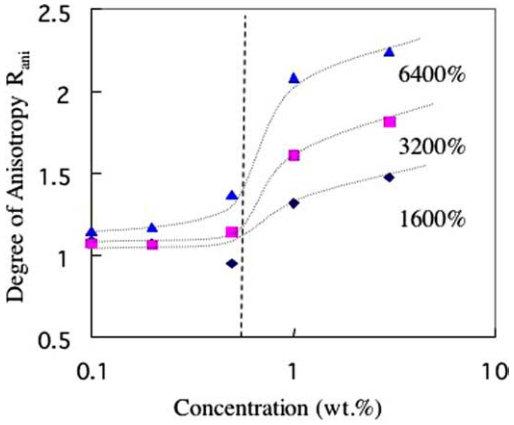

Fig. 7. Degree of anisotropy R_{ani} as a function of the concentration of HMW PE. Shear rate $\dot{\gamma}=4\ s^{-1}$, shear strain $\varepsilon=1600$, 3200 and 6400%.

concentration, showing that there is a threshold for the anisotropy at around $C^*_{ani}=0.5$–0.6 wt%. It should be noted that the threshold is almost independent of the shear strain although the degree of anisotropy increases with the shear strain. This gives us a hint to consider the physical meaning of the threshold for the anisotropy C^*_{ani}.

We compare the threshold concentration C^*_{ani} to the chain overlap concentration $C^*_{R_g}$ of the HMW PE. The overlap concentration of polymer chains with radius of gyration R_g is given by

$$C^*_{R_g}=\frac{M_w}{(4/3)\pi\langle R_g^2\rangle^{3/2}N_A} \tag{1}$$

where $\langle R_g^2\rangle$ is the mean square radius of gyration of the polymer chain, which is given by Eq. (2) under the Gaussian chain approximation with molecular weight distribution $U=M_w/M_n-1$ (Ref. [38])

$$\langle R_g^2\rangle=\frac{bL(2U+1)}{3(U+1)} \tag{2}$$

where b and L are the persistence length and the contour length. Taking the literature data $[\langle R_g^2\rangle/M_w]^{1/2}=0.46$ [35], we have calculated the overlap concentration $C^*_{R_g}$ to be 0.178 g/cm^3 or 0.209 wt%, which is smaller than the threshold concentration. The ratio of the threshold concentration to the overlap concentration $C^*_{ani}/C^*_{R_g}$ is 2.5–3. This strongly suggests that entanglements of the HMW PE are very important for the formation of the shish-like structure. This agrees qualitatively with the finding of Kornfield et al. [32] that the role of the long chain in the shear-induced crystallization is cooperative rather than a single chain event. Note that the threshold in their experiment is slightly lower than the present one. We used PEs with rather broad molecular weight distributions, and it may make the threshold apparently higher because entanglements are more effective in higher molecular weight. This must be a cause for the small quantitative disagreement. The present result can be understood in the following picture. In order to produce the shish-like structure polymer chains must be extended due to the shear. Suppose that the HMW PE are isolated in the blend, they are somewhat extended by the shear flow, however, it does not lead to the anisotropic structure formation as seen in Fig. 6. On the other hand, when the concentration of HMW PE is above a threshold for entanglements, the chains must be extended due to the connectivity as polymer network is deformed. The threshold for the anisotropy C^*_{ani} must correspond to the concentration above which entanglements work effectively. This is schematically illustrated in Fig. 8(a) and (b). This picture reminds us

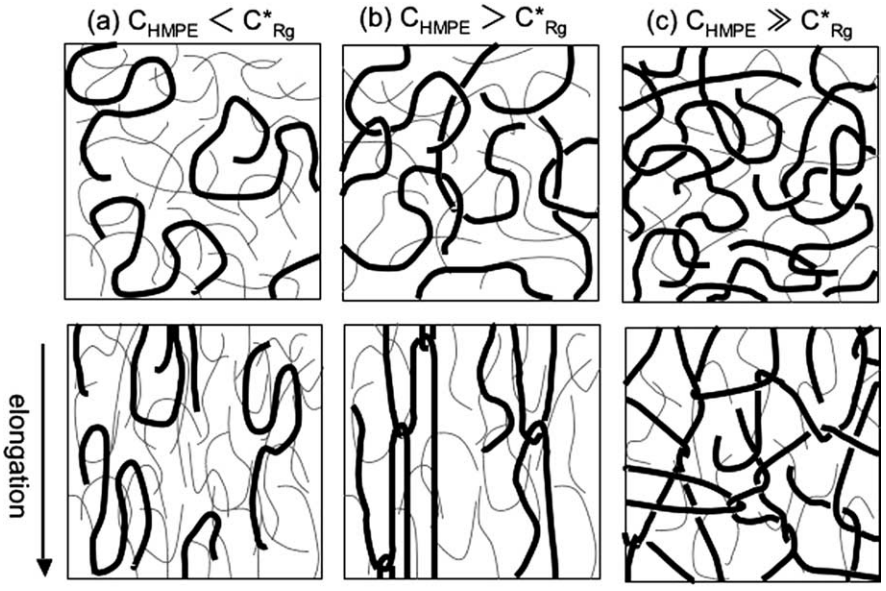

Fig. 8. Schematic illustrations of the role of HMW PE in formation of shish-like structure. Thin and thick curves represent HMW and LMW PEs, respectively. (a) $C_{HMPE}<C^*_{R_g}$: HMW PE chains are isolated and slightly extended by the shear, (b) $C_{HMPE}>C^*_{R_g}$: HMW PE chains are entangled and extended due to the connectivity as polymer network is deformed, (c) $C_{HMPE}\gg C^*_{R_g}$: too many cross-linking points (or entanglements) prevent extension of HMW PE chains.

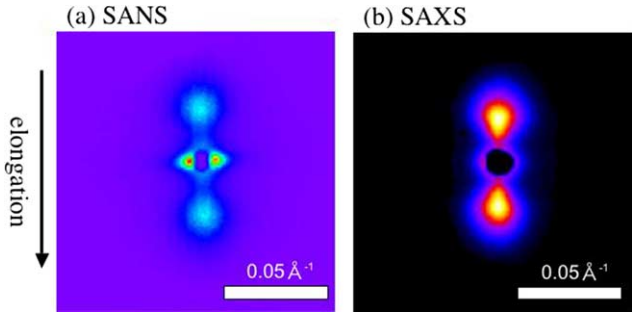

Fig. 9. 2D SANS (a) and 2D SAXS (b) patterns from an elongated blend of LMW deuterated PE and HMW hydrogenated PE (3 wt%).

the gel-spinning technique [39–42] to produce ultra-high strength and ultra-high modulus fiber of PE although all of the situations are not the same. In this procedure, PE chains are extremely extended because the tension is transmitted though the cross-linking points in the gel network. On the other hand, in order to obtain the ultra-high strength fiber the number of the cross-linking points should be as little as possible because too many cross-linking points prevent the extension of polymer chains. It is therefore, expected in the crystallization of the PE blend under shear flow that formation of the shish-like structure is suppressed at a rather high concentration of the HMW PE above C^*_{ani} because the polymer chains cannot be extended due the shear because of too many entanglements as illustrated in Fig. 8(c).

3.2. SANS and SAXS measurements

The DPLS measurements indicated that the formation of shish-like structure is enhanced by addition of the HMW component. It is therefore, expected that the shish-like structure is mainly formed from the HMW PE. However, it has not been directly confirmed in the experiments. Furthermore, in small-angle X-ray scattering (SAXS) measurements [12,43] the shish-like structure was not always observed even though the shear condition was stronger than in the present experiment. When no shish-like structure is observed, many interpretations are possible, e.g. the shish-like structure is once formed but it disappears immediately after the formation; the number of the shish is too little to be detected within sensitivity of SAXS; the length of the shish is too long to be detected within the SAXS resolution. In order to shed light on these problems, we have performed SANS and SAXS measurements on an elongated blend of HMW hydrogenated PE (3 wt%) with $M_w = 2{,}000{,}000$ and LMW deuterated PE with $M_w = 200{,}000$. This experiment is on the basis of the following idea. From the results of the DPLS measurements, we expect that the shish-like structure is mainly formed from the HMW hydrogenated PE. It is well known in SANS that scattering contrast between hydrogenated and deterated PEs is very large [44], so that we can observe the shish-like structure if it is formed from the HMW hydrogenated PE due to the high scattering contrast. On the other hand, in SAXS scattering contrast arises form electron density difference, which corresponds to mass density difference in one component systems. Therefore, we expect very large difference between SANS and SAXS scattering profiles. However, if the HMW hydorogenated PE chains are homogeneously distributed in the shish and the kebab structure, SANS scattering contrast in the small-angle region arises only from the density difference similar to SAXS. In this case, we expect that the scattering patterns are almost the same in both of SANS and SAXS. Hence, we can see whether or not the shish is mainly formed from the HMW PE by comparing SANS data to SAXS data.

The observed 2D SANS pattern is shown in Fig. 9(a). Very strong streak-like scattering intensity is observed along the direction normal to the elongation in the low Q range, suggesting that the shish structure is formed during the elongation process. Two-spot scattering pattern is also observed in the direction parallel to the elongation. This must correspond to the spacing between the neighboring kebabs (lamellar crystalline structure) periodically attached along the shish. The scattering contrast seems very large in the streak-like scattering compared to the two-spot scattering. In order to see it quantitatively, the sector averaged scattering intensities

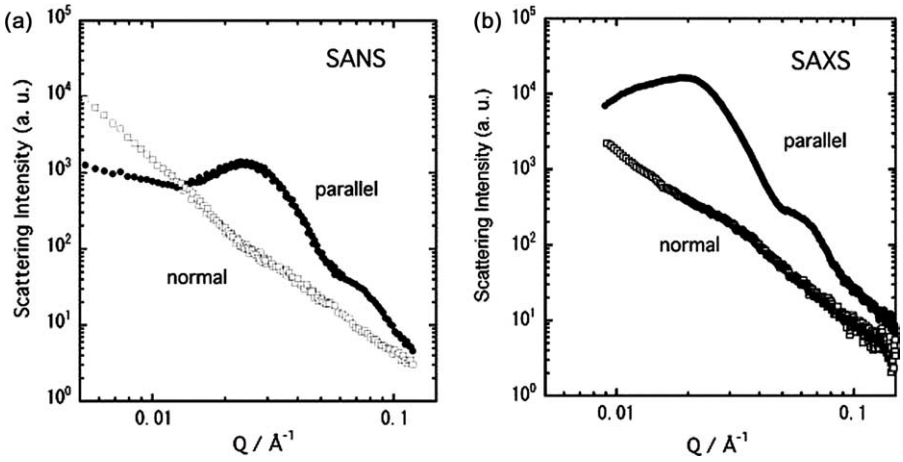

Fig. 10. Sector averaged SANS (a) and SAXS (b) intensities from an elongated blend of LMW deuterated PE and HMW hydrogenated PE (3 wt%) in directions normal and parallel to the elongation.

in azimuthal angle ranges between −5° and +5 and between 85 and 95° are plotted against Q in Fig. 10(a), where the azimuthal angle of 0° corresponds to the elongational direction. In the direction normal to the elongation the scattering intensity has no peaks and is very strong in the low Q range below about 0.02 $Å^{-1}$. On the other hand, the intensity parallel to the elongation shows a peak at around $Q=0.025$ $Å^{-1}$, corresponding to the spacing between the neighboring kebabs. What we have to emphasize here is that the intensity from the shish below about 0.01 $Å^{-1}$ is much stronger than that from the kebab, showing the high scattering contrast of the shish. This implies that the shish structure is mainly formed from the HMW hydrogenated PE and the kebab is formed from the LMW deuterated PE.

Small-angle X-ray scattering (SAXS) measurements were also performed on the same sample in the SR facility, SPring-8 in Nishiharima, and the observed 2D scattering pattern is shown in Fig. 9(b). In contrast to the SANS result, the streak-like scattering due to the shish structure was not observed although the two-spot pattern due to the spacing between the kebabs was clearly observed in the direction parallel to the elongation. The sector averaged SAXS intensities are also shown in Fig. 10(b) in azimuthal angle ranges between −5° and +5 and between 85 and 95°. The scattering intensity parallel to the elongation shows a peak corresponding to the kebab spacing similar to the SANS result. On the other hand, the intensity normal to the elongation is very weak, particularly in the low Q range below about 0.02 $Å^{-1}$ in contrast to the SANS data. As seen in the SANS data the shish structure is certainly present in the elongated blend, however, the shish structure is not observed in the SAXS measurement. In combination of the SANS and SAXS results, we can directly conclude that the shish is mainly formed from the HMW component and the number of shish is too little to be detected within the present SAXS sensitivity.

4. Conclusion

We have studied the crystallization process of blends of HMW polyethylene (PE) and LMW PE under shear flow using DPLS with the pulse shear technique as a function of concentration of HMW PE in a range of 0–3 wt%, focusing on effects of the HMW PE on the shish-like structure formation. It was found that the shish-like structure formation is enhanced by the HMW component above a threshold concentration C^*_{ani} of the HMW PE. This threshold is 2.5–3 times larger than the chain overlap concentration $C^*_{R_g}$, suggesting that entanglements of HMW PE chains play an essential role for the formation of shish-like structure. On the basis of the results, it was suggested that a gel-spinning-like mechanism for the shish-like structure formation. The DPLS results also suggest that the shish-like structure is formed from the HMW component. In order to confirm it we performed the small-angle neutron scattering (SANS) and X-ray scattering (SAXS) measurements on the elongated blend of the HMW hydrogenated PE (3 wt%) and LMW deuterated PE. In the SANS streak-like scattering due to the shish structure was clearly observed in the direction normal to the elongation although it was absent in the SAXS. This is due to the high neutron scattering contrast between the hydrogenated and deuterated PE, confirming that the shish structure is mainly formed from the HMW PE and the number of the shish is too little to be detected within the present SAXS sensitivity.

Acknowledgements

We are grateful to Prof Kaji for valuable discussions. We also thank to Prof Shibayama for the support of the SANS measurements, and to Dr. Fujisawa for the support of the SAXS measurements.

References

[1] Pennings AJ, Kiel AM, Colloid ZZ. Polym 1965;205:160–2.
[2] Pennings AJ. J Polym Sci, Part C: Polym Symp 1977;59:55–86.
[3] Odell JA, Grubb DT, Keller A. Polymer 1978;19:617–26.
[4] Bashir Z, Odell JA, Keller A. J Mater Sci 1984;19:3713–25.
[5] Bashir Z, Odell JA, Keller A. J Mater Sci 1986;21:3993–4002.
[6] Keller A, Kolnaar JWH. In: Meijer HEH, editor. Processing of polymers. New York: VCH; 1997. p. 189–268.
[7] Ward IM. Structure and properties of oriented polymers. New York: Wiley; 1975.
[8] Ziabicki A. Fundamentals of fiber formation. New York: Wiley; 1976.
[9] Walczak ZK. In: Processses of fiber formation. Amsterdam: Elsevier; 2002.
[10] Samon JM, schultz JM, Hsiao BS, Seifert S, Stribeck N, Gurke I, et al. Macromolecules 1999;32:8121–32.
[11] Samon JM, Schultz JM, Wu J, Hsiao BS, Yeh F, Kolb R. J Polym Sci, Part B: Polym Phys 1999;37:1277–87.
[12] Somani RH, Hsiao BS, Nogales A, Srinivas S, Tsuo AH, Sics I, et al. Macromolecules 2000;33:9385–94.
[13] Schultz JM, Hsiao BS, Samon JM. Polymer 2000;41:8887–95.
[14] Samon JM, Schultz JM, Hsiao BS, Wu J, Khot S. J Polym Sci, Part B: Polym Phys 2000;38:1872–82.
[15] Samon JM, Schultz JM, Hsiao BS, Khot S, Johnson HR. Polymer 2001; 42:1547–59.
[16] Nogales A, Somani RH, Hsiao BS, Srinivas S, Tsuo AH, Balta-Calleja J, et al. Polymer 2001;42:5247–56.
[17] Somani RH, Hsiao BS, Nogales A, Fruitwala H, Srinivas S, Tsuo AH. Macromolecules 2001;34:5902–9.
[18] Somani RH, Young L, Hsiao BH, Agarwal PK, Fruitwala HA, Tsuo AH. Macromolecules 2002;35:9096–104.
[19] Somani RH, Yang L, Hsiao BS. Physica A 2002;304:145–57.
[20] Yang L, Somani RH, Sics I, Hsiao BH, Kolb R, Fruitwala H, et al. Macromolecules 2004;37:4845–59.
[21] Pogodina NV, Siddiquee SK, Egmond JWV, Winter HH. Macromolecules 1999;32:1167–74.
[22] Pogodina NV, Lavrenko VP, Srinivas S, Winter HH. Polymer 2001;42: 9031–43.
[23] Elmoumni A, Winter HH, Waddon AJ, Fruitwala H. Macromolecules 2003;36:6453–61.
[24] Kumaraswamy G, Issaian AM, Kornfield JA. Macromolecules 1999;32: 7537–47.
[25] Kumaraswamy G, Verma RK, Issaian AM, Wang P, Kornfield JA, Yeh F, et al. Polymer 2000;41:8934–40.
[26] Kumaraswamy G, Kornfield JA, Yeh F, Hsiao B. Macromolecules 2002; 35:1762–9.
[27] Fukushiam H, Ogino Y, Matsuba G, Nishida K, Kanaya T. Polymer 2005; 46:1878–85.

[28] Sherwood CH, Price FP, Stein RS. J Polym Sci Polym Symp 1978;63: 77–94.
[29] Lagasse RR, Maxwell B. Polym Eng Sci 1976;16:189–203.
[30] Vleeshouwers S, Meijer H. Rheol Acta 1996;35:391–9.
[31] Keller A, Odell JA. Colloid Polym Sci 1985;263:181–201.
[32] Seki M, Thurman DW, Oberhauser JP, Kornfield J. Macromolecules 2002;35:2583–94.
[33] Schelten J, Wignall GD, Ballard DGH. Polymer 1974;15:682–5.
[34] Schelten J, Wignall GD, Ballard DGH, Schmatz W. Colloid Polym Sci 1974;252:749–52.
[35] Schelten J, Ballard DGH, Wignall GD, Longman G, Schmatz W. Polymer 1976;17:751–7.
[36] Ito Y, Imai M, Takahashi S. Physica B 1995;213/214:889–91.
[37] Fujisawa T, Inoue K, Oka T, Iwamoto H, Uruga T, Kumasaka T, et al. J Appl Crsyt 2000;33:797–800.
[38] Oberthuer RC. Makromol Chem 1978;179:2693–706.
[39] Smith P, Lemstra PJ, Kalb B, Pennings AJ. Polym Bull 1979;1:733–6.
[40] Smith P, Lemstra PJ. J Mater Sci 1980;15:505–14.
[41] Lemstra PJ, Aerle NAJMv, Bastiaansen CWM. Polym J 1987;19: 85–98.
[42] Bastiaansen CWM. J Polym Sci: Polym Phys 1990;28:1475–82.
[43] Liangbin L. Jeu WHd. Macromolecules 2003;36:4862–7.
[44] Higgins JS, Benoit HC. Polymers and Neutron Scattering. Oxford: Clarendon Press; 1994.